This paper is published as part of a *Dalton Transactions* themed issue on:

Supramolecular photochemistry

Guest Editors Michael D. Ward and Julia Weinstein
University of Sheffield, UK

Published in issue 20, 2009 of *Dalton Transactions*

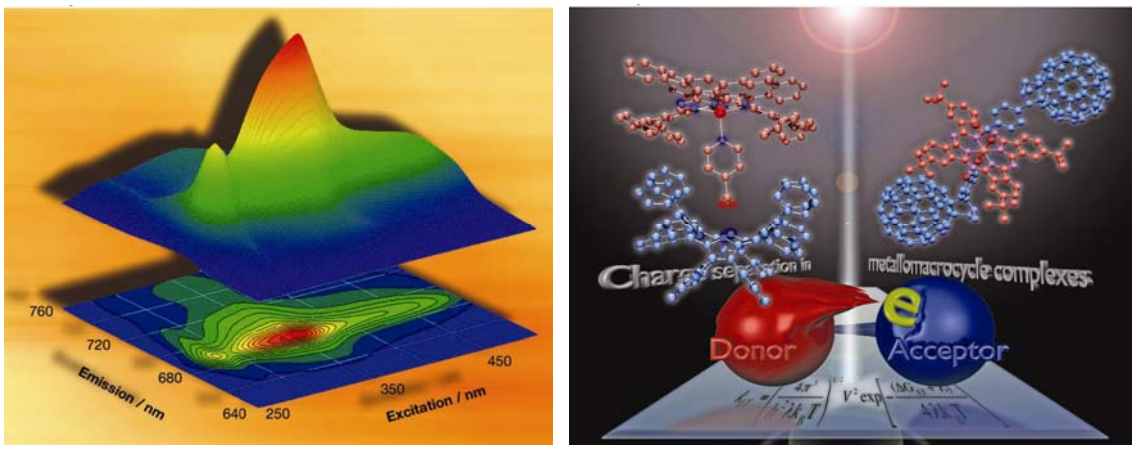

Images reproduced with permission of U. Nickel (left) and Shunichi Fukuzumi (right)

Papers published in this issue include:

Perspective: Sensitised luminescence in lanthanide containing arrays and d–f hybrids
Stephen Faulkner, Louise S. Natrajan, William S. Perry and Daniel Sykes, *Dalton Trans*., 2009, DOI: 10.1039/b902006c

[Pt(mesBIAN)(tda)]: A near-infrared emitter and singlet oxygen sensitizer
Aaron A. Rachford, Fei Hua, Christopher J. Adams and Felix N. Castellano, *Dalton Trans*., 2009, DOI: 10.1039/b818177b

Self-assembly of double-decker cages induced by coordination of perylene bisimide with a trimeric Zn porphyrin: study of the electron transfer dynamics between the two photoactive components
Ana I. Oliva, Barbara Ventura, Frank Würthner, Amaya Camara-Campos, Christopher A. Hunter, Pablo Ballester and Lucia Flamigni, *Dalton Trans.*, 2009, DOI: 10.1039/b819496c

Synthesis, photophysical and electrochemical characterization of phthalocyanine-based poly(*p*-phenylenevinylene) oligomers
Juan-José Cid, Christian Ehli, Carmen Atienza-Castellanos, Andreas Gouloumis, Eva-María Maya, Purificación Vázquez, Tomás Torres and Dirk M. Guldi, *Dalton Trans.*, 2009, DOI: 10.1039/b818772j

Luminescence, electrochemistry and host–guest properties of dinuclear platinum(II) terpyridyl complexes of sulfur-containing bridging ligands
Rowena Pui-Ling Tang, Keith Man-Chung Wong, Nianyong Zhu and Vivian Wing-Wah Yam, *Dalton Trans.*, 2009, DOI: 10.1039/b821264c

Visit the *Dalton Transactions* website for more cutting-edge inorganic and organometallic research
www.rsc.org/dalton

Chiral photochemistry within a confined space: diastereoselective photorearrangements of a tropolone and a cyclohexadienone included in a synthetic cavitand†

Arun Kumar Sundaresan,[a] Lakshmi S. Kaanumalle,[a] Corinne L. D. Gibb,[b] Bruce C. Gibb[b] and V. Ramamurthy*[a]

Received 6th January 2009, Accepted 25th February 2009
First published as an Advance Article on the web 31st March 2009
DOI: 10.1039/b900017h

The value of a supramolecular assembly to enforce a closer interaction between a chiral auxiliary and a reaction center has been established using photoreactions of tropolone and cyclohexadienone derivatives. Two probe molecules utilized to establish the concept undergo 4 e– electrocyclization and oxa-di-π-methane rearrangement from excited singlet and triplet state, respectively. The chiral auxiliaries investigated here has no/little effect in acetonitrile solution during phototransformations of the probe molecules to yield products with new chiral centers. On the other hand the same ones are able to enforce diastereoselectivities to the extent of ~30% when the reactions occur within the restricted space of a capsule made up of a synthetic cavitand commonly known as octa acid. Extensive NMR studies have been utilized to characterize the guest–host supramolecular structures. The results presented here should be of value in the overall understanding of chiral induction in photochemical reactions.

Introduction

Several strategies have been employed to effect chiral induction in asymmetric photoreactions.[1] Photoreactions have been carried out in solid phase, solution phase and in organized assemblies. The chiral sources employed include circularly polarized light, chiral sensitizers, chiral solvents, chiral substituents, chiral host–guest assemblies and chiral crystalline environments.[2,3] In each method, chiral information is transferred to a prochiral or a racemic substrate through non-covalent interactions, allowing chiral amplification. In recent years we have successfully applied two techniques, chiral inductor and chiral auxiliary, to achieve chiral induction in a variety of photoreactions within zeolites.[4,5] In the chiral inductor approach, both the chiral molecule and the substrate are confined to the same reaction site of a supramolecular host. In the chiral auxiliary approach, the substrate and the chiral molecule are covalently linked. When the chiral auxiliary is linked to the substrate, they are forced to be in close contact within the confined space of a zeolite and hence this method is generally more effective than the chiral inductor method. Photochemical reactions using both these methods are reported by several groups in crystalline state as well as in solid-state host–guest assemblies with considerable success.[6–9]

In this manuscript, we highlight results of our studies in host–guest assemblies in aqueous medium using photocylization of a tropolone ether and oxa-di-π-methane rearrangement of a cyclohexadienone.[10–13] The host used is a synthetically available cavitand commonly known as octa acid (OA).[14,15] The size and shape of this host is compared in Scheme 1 with that of cyclodextrin (CD) and cucurbituril (CB) that are more known to photochemists. The main difference between OA and the other two hosts is that OA forms a capsule surrounding one or two guest molecules.[16–18] Results presented here must be viewed from the context that even with cyclodextrin the best chiral induction in photochemical reactions is less than 30% (diastereomeric excess *via* chiral auxiliary strategy and enantiomeric excess *via* chiral inductors strategy where CD is the chiral inductor).[19–24] Usefulness of cucurbiturils in chiral photochemistry has not yet been established. Further, unlike thermal reactions, rules of chiral induction in photochemical reactions are yet to be understood and results presented here, we believe, would help construct a model that would enable one predict in due course the factors that need to be controlled to achieve chiral induction in photoreactions. The current study consists of NMR characterization and photochemical investigation of host–guest complexes.

The two systems, tropolone ether **1** and cyclohexadienone **2**, we have examined in the context of chiral induction within OA capsule are represented in Scheme 2. In both cases a chiral auxiliary is covalently placed far removed from the reaction site. The chiral auxiliary thus placed has very little effect during photoreaction in solution (diastereomeric excess, de < 3%). Thus the chemistry in solution was used as the standard to compare the results in guest–OA complex.

Chiral products from achiral tropolone ether arise *via* a 4-electron disrotatory cyclization process. Two of the three π-bonds of tropolone undergo concerted cyclization reaction to yield the bicyclic products **3** and **3a** shown in Scheme 3. The cyclization can occur along two different faces of the planar molecule and can follow paths A or B in Scheme 3. The newly formed four membered ring is either below (path A) or above (path B) the plane of the five membered ring and yields photoproducts **3** and **3a**, respectively, in Scheme 3. As illustrated

[a]*Department of Chemistry, University of Miami, Coral Gables, FL 33124, USA. E-mail: murthy1@miami.edu*
[b]*Department of Chemistry, University of New Orleans, New Orleans, LA 70148, USA*

† Electronic supplementary information (ESI) available: Additional NMR spectra. See DOI: 10.1039/b900017h

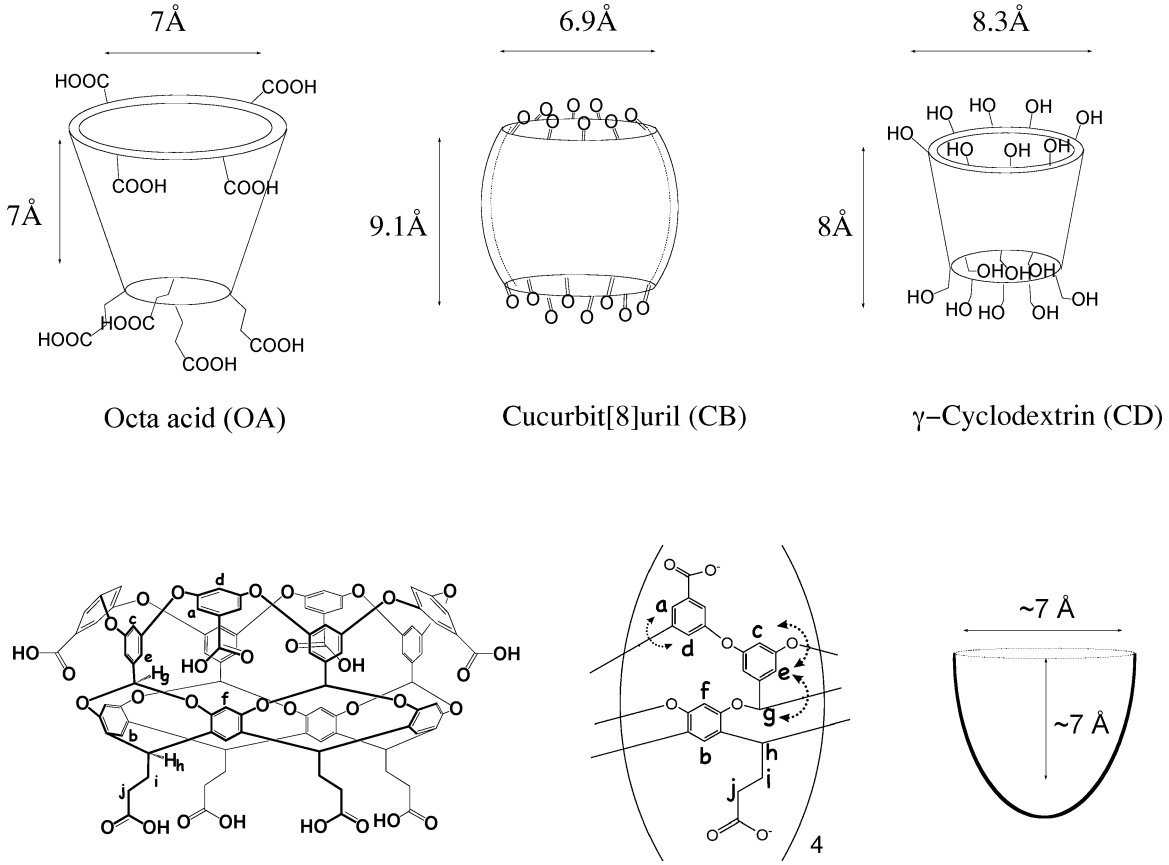

Scheme 1 Pictorial representation of the structures of octa acid, cucurbit[8]uril and γ-cyclodextrin showing the relative dimensions of the host cavity.

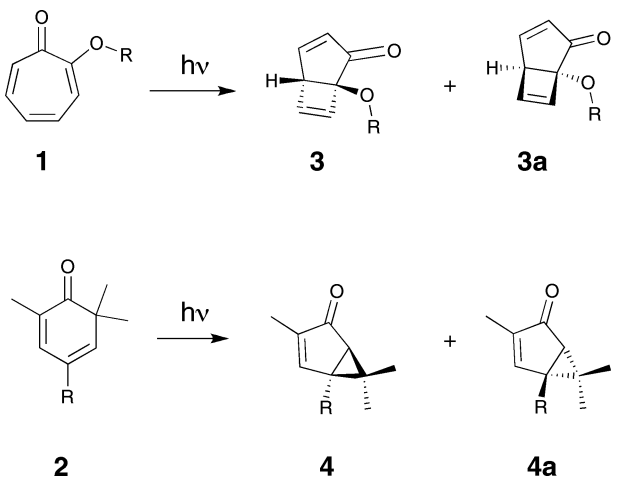

Scheme 2 Structures of the substrates investigated and their primary photoproducts.

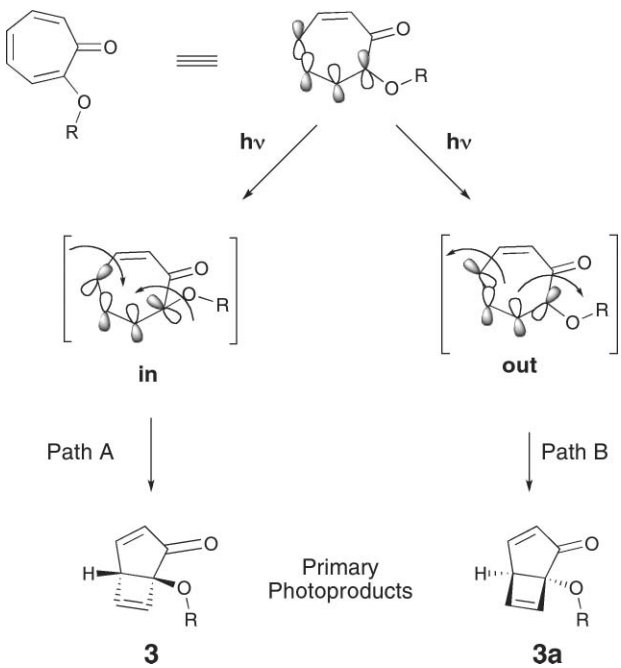

Scheme 3 The 4-electron disrotatory cyclization reaction of tropolone ether yielding two chiral photoproducts.

in Scheme 4, 3,3,5-trimethyl-4-oxocyclohexa-1,5-dienecarboxylic acid undergoes oxa-di-π-methane rearrangement to yield bicyclic products **4** and **4a** The reaction proceeding *via* triplet state involves formation of 1,5-diradical intermediate. Analogous to the cyclization reaction of tropolone ethers, the photoproduct can cyclize along either face of the five-membered cyclic intermediate to yield a pair of enantiomers. In the current examples (**1** and **2**) we envision that differences in the interaction between chiral auxiliary and the two faces of tropolone or cyclohexadienone would either impede one reaction pathway or facilitate one pathway and thus yield excess of one of the photoproducts. The belief that within a confined space one could force stronger interaction between a

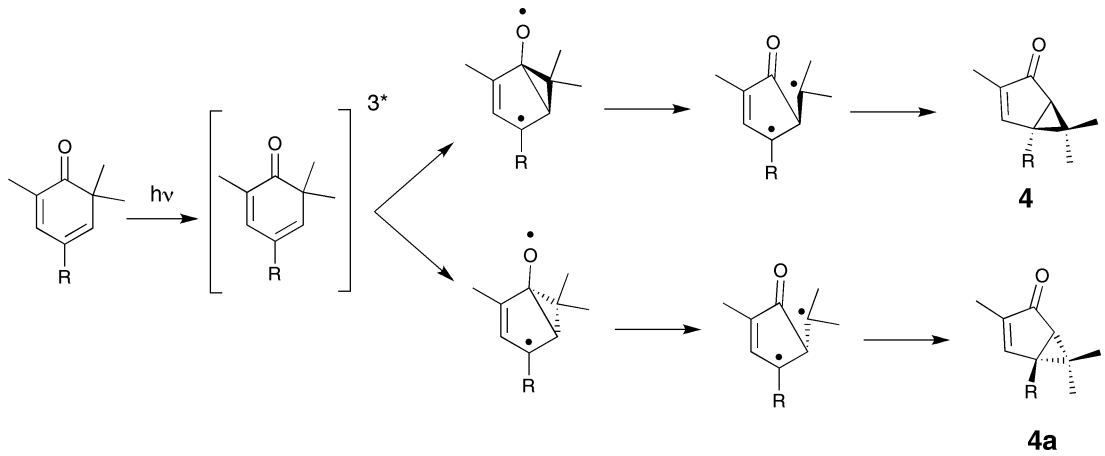

Scheme 4 Mechanism of the oxa-di-π-methane rearrangement of a dienone.

chiral auxiliary and the reaction site than in a free solution has prompted the current investigation.

Results and discussion

NMR characterization of reactant–OA complexes

Octa acid and tropolone ether **1** and cyclohexadienone derivative **2** formed complexes in 2 : 1 ratio in buffered aqueous solution. ^{1}H NMR spectrum, 1D selective total correlation spectroscopy (TOCSY) NMR spectra, nuclear Overhauser effect spectroscopy (NOESY) NMR spectrum and diffusion ordered spectroscopy (DOSY) NMR spectrum of **1**@OA_2 are shown in Fig. 2–6. ^{1}H NMR, COSY and NOESY NMR spectra of OA complex of **2** are provided in Fig. 8–11. A detailed discussion of the NMR analyses of OA and tropolone ether **1** complex is provided below followed by a brief discussion on OA and cyclohexadienone derivative **2**.

In ^{1}H NMR spectrum of **1**@OA_2 shown in Fig. 1, first, consider the signals of the host. The aromatic signals of OA were split after addition of **1**. Before embarking on the analyses of the spectra we recognize that in theory the signals from H-b, c, d, f and g should each appear as two signals because in the capsule the northern hemisphere and the southern hemisphere of the host are not the same (they are binding different parts of the guest). Furthermore, because the guest is chiral, H-a and e are diastereomeric in the complex; they are non-equivalent. Thus, for example, the two H-e protons in one hemisphere are non-equivalent, and both are different from the non-equivalent H-e signals in the other hemisphere. Thus, for both H-e and H-a there could be four signals. Sometimes, because of coincidence, these splitting patterns may not be apparent.

1D selective TOCSY NMR spectra provided in Fig. 2 and 3 for OA and OA-**1** complex helped in identifying the host signals. In the TOCSY NMR of free OA, (Fig. 2), selective irradiation of each

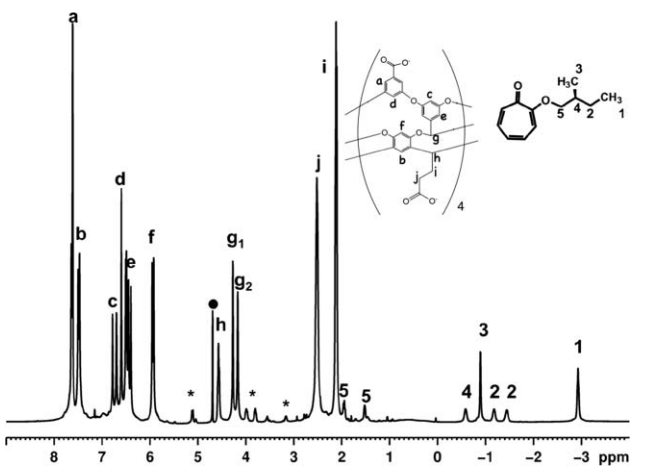

Fig. 1 ^{1}H NMR spectrum (500 MHz, D_2O, 2.5×10^{-3} M **1**, 5×10^{-3} M OA, 5×10^{-2} M sodium tetraborate, 298 K) of **1**@OA_2 complex. Octa acid signals are labelled (a–j) and guest aliphatic signals are labelled (1–5). Other guest signals are indicated with *. Residual water signal is indicated with ●.

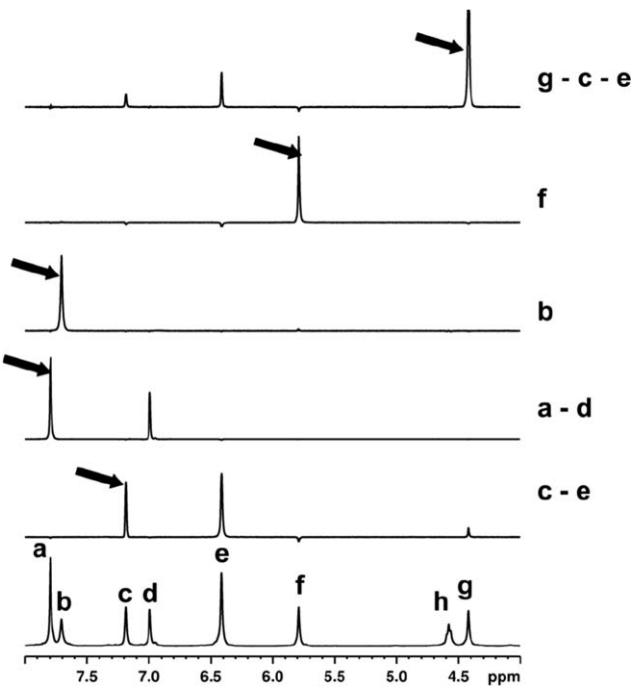

Fig. 2 Top: 1D selective TOCSY NMR spectra of octa acid (500 MHz, DMSO-d_6, 0.12 s mixing time). Irradiated signals are marked with an arrow. Refer structure of OA in Scheme 1 for the correlations.

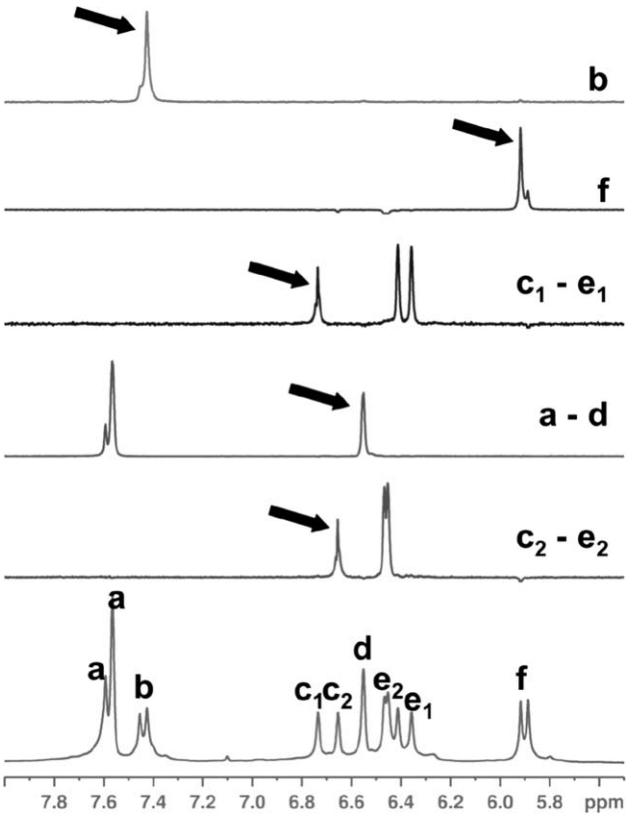

Fig. 3 1D selective TOCSY NMR spectra of **1**@OA_2 (500 MHz, D_2O, 2.5×10^{-3} M **1**, 5×10^{-3} M OA, 5×10^{-2} M sodium tetraborate 0.12 s mixing time). Irradiated signals are marked with an arrow. Correlations are based on TOCSY NMR of octa acid shown in Fig. 2.

host signal was carried out. The resultant NMR spectrum showed the signals of the covalently linked hydrogens of the host. For example, irradiation at 7.8 ppm (signal a in Fig. 2, corresponding to H_a of OA) showed one additional signal and was assigned as H_d, which is present in the same ring as H_a. In the TOCSY NMR of OA–**1** complex shown in Fig. 3, irradiation of the H_d signal at 6.55 ppm showed the H_a signal at 7.6 ppm. Similarly, H_c and H_e hydrogen atoms of OA that are in the same ring show TOCSY correlations and were identified in the NMR of the complex. Signals of H_b and H_f atoms did not show TOCSY correlations, although they are in the same ring. By comparing the TOCSY NMR of free OA and the TOCSY NMR of OA–**1** complex, all the signals of the host were assigned. In the NMR spectrum of the complex, the diastereotopic H_a signals of the host were spilt into two, and so were H_b, H_c, and H_f signals. H_e signals were split into two doublets in the NMR spectrum of the complex. The additional observation in the 1D TOCSY correlation of the complex **1**@OA_2 was that while H_c and H_e signals showed TOCSY correlations, no TOCSY correlation was observed between the two H_c signals (c_1 and c_2 in Fig. 3). Similarly, two sets of H_e signals (marked e_1 and e_2 in Fig. 3) did not show through bond connectivity. That is, the two sets of hydrogens H_{c1} and H_{e1}, and H_{c2} and H_{e2} were not covalently linked. Generally, split signals originate from the two host molecules that constitute the complex. Since they bind to different portions of the guest, their signals are affected by the guest in different manner and are observed as split signals. Thus based on the TOCSY information, it can be confirmed that the two sets of signals corresponding to H_c and H_e originate from two different octa acid molecules.

Aliphatic group signals of the guest in **1**@OA_2 are shifted below 0 ppm due to the shielding effect of the aromatic rings of the host. The 3.8 ppm and 2 ppm upfield shift of CH_3 signals '1' and '3', respectively, is an illustration of the greater, differential shielding of the guest at the tapering end of the capsule than its wider 'equatorial region. TOCSY NMR spectrum shown in Fig. 4 revealed all the aliphatic signals of the guest. Olefinic signals of the guest were observed at 5.1 ppm, 4 ppm 3.8 ppm and 3.2 ppm and are marked with * in Fig. 1.

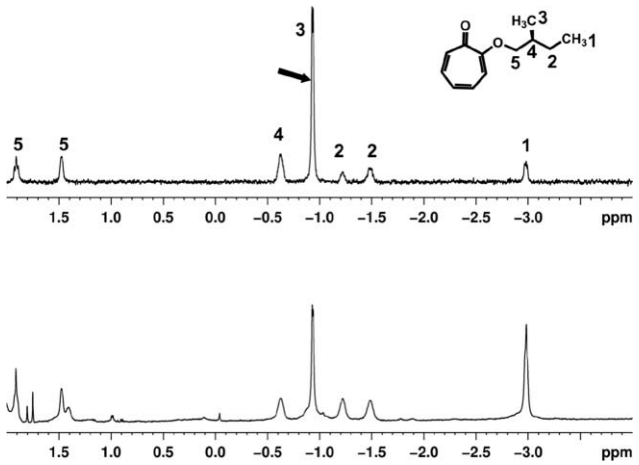

Fig. 4 1D selective TOCSY NMR spectrum (top) and 1D NMR spectrum (bottom) of **1**@OA_2 (500 MHz, D_2O, 2.5×10^{-3} M **1**, 5×10^{-3} M OA, 5×10^{-2} M sodium tetraborate, 0.12 s mixing time). Irradiated signal is marked with an arrow.

Additionally, 2D NOESY NMR of the complex was performed to obtain through space interactions between the host and the guest. NOESY spectrum showed strong correlations between the more shielded (terminal) methyl hydrogens of the guest (signal 1 in Fig. 5) and only one H_g signal of the host. In addition to host–guest correlations, intramolecular NOE interactions between the guests' signals was evident in the NOESY analysis. In the ^1H NMR spectrum, the methylene signals (signals '2' and '5' in Fig. 1 and 4) were split into two. NOE correlation between the two methylene hydrogens of signal 2 was evident in the NOESY spectrum (marked with dotted lines in Fig. 5).

Diffusion coefficient of the complex was determined by DOSY NMR analysis (Fig. 6) and was calculated to be 1.26×10^{-10} m^2s^{-1}. In the DOSY NMR spectrum of the complex shown in Fig. 6, both the octa acid signals and the guest signals posses identical diffusion coefficients confirming that the complex is stable during the experiment time period. For comparison, the diffusion coefficient of the water signal (at 4.8 ppm) is much higher than that of the complex. Since the diffusion coefficient is a function of the size of the molecule, presence of free (unbound) guest will be revealed in the DOSY spectrum, as free guest will have a greater rate of diffusion. Hence, based on DOSY NMR analysis, it can be concluded that the complex of octa acid and **1** is stable and the complex is either a 2 : 1 or 2 : 2 complex.[25–27] Due to solubility problems, proper titration experiments could not be carried out both in the case of **1** and **2**. However, when the guest concentration is greater than 0.5 equiv. with respect to the host,

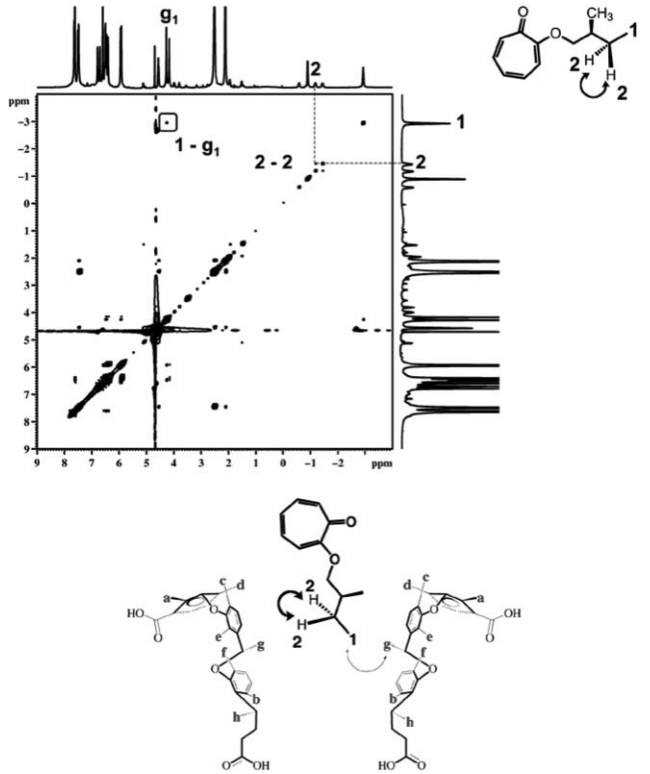

Fig. 5 NOESY NMR spectrum (500 MHz, D_2O, 298 K, 2.5×10^{-3} M **1**, 5×10^{-3} M OA, 5×10^{-2} M sodium tetraborate, 0.5 s mixing time) of the **1**@OA_2 complex. Correlation between guest methyl and host's H_g, and correlation between the two guest H_2 signals are highlighted.

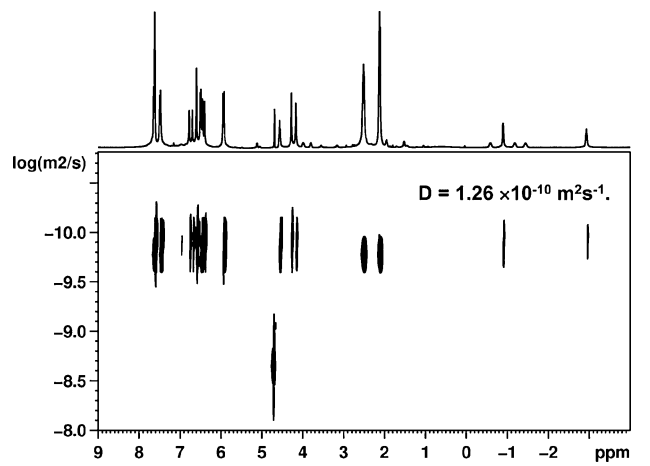

Fig. 6 DOSY NMR spectrum (500 MHz, D_2O, 2.5×10^{-3} M **1**, 5×10^{-3} M OA, 5×10^{-2} M sodium tetraborate) of **1**@OA_2 complex. The calculated diffusion coefficient is 1.26×10^{-10} m^2s^{-1}.

the clear solution turns turbid and gradual precipitation of free guest is visibly clear when excess guest is added. This suggested that the host–guest ratio is 2 : 1 and not 2 : 2. We were not able to generate a Job-plot to obtain the exact host–guest ratio for the following reason. Job-plot is an effective method of depicting the host–guest binding behaviour when there is a gradual change in the NMR shift with gradual addition of the host. Since the guest was not water soluble no signal due to free guest was evident and only signals seen were due to the bound guest. This alone is not sufficient to generate a Job-plot.

Similar analyses of the complex between OA and **2** revealed it to be a 2 : 1 complex. The stoichiometry of the complex was established by integration of the NMR spectrum shown in Fig. 7. DOSY NMR of 5×10^{-3} M solution of the **2**-OA complex showed it to have a diffusion coefficient of 1.26×10^{-10} m^2s^{-1}, comparable to complex **1**@OA_2. The stability of the complex was also established by way of identical diffusion coefficients for both the guest and the host.

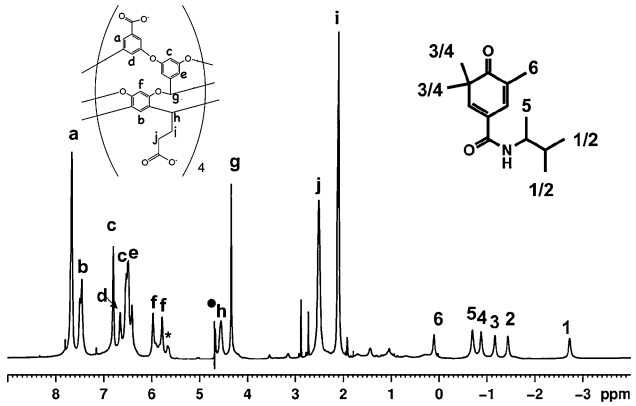

Fig. 7 ^{1}H NMR spectrum (500 MHz, D_2O, 298 K, 2.5×10^{-3} M **2**, 5×10^{-3} M OA, 5×10^{-2} M sodium tetraborate) of **2**@OA_2 complex. Host signals are labelled (a–j). Guest methyl signals are numbered and the residual water signal is marked with ●.

Similar to the OA complex with **1**, signals of both the host and the guest were affected upon binding. All the aromatic signals of OA were split upon binding of the guest. Analysis of the guest signals of OA bound **2** was performed based on COSY and NOESY NMR along with ^{1}H NMR chemical shifts. Compound **2** possesses six methyl groups, of which two are geminal methyl groups. Consequently, only four signals were observed when the NMR spectrum of **2** was recorded in $CDCl_3$. 1D TOCSY analysis of the guest signals (spectrum not shown) did not show any correlations, and were not useful in assigning the guest signals. COSY spectrum (Fig. 9) helped us to assign the methyl signals of the guest. ^{1}H NMR of **2**@OA_2 complex showed six distinct signals of equal intensity, one for each CH_3 group (signals 1–6 in Fig. 7). Not only were they distinct, chemical shift difference between the first and the last signal was 2.8 ppm. Even two sets of geminal dimethyl signals are well separated after binding to OA. Of the two geminal methyl groups, chemical shift of the most shielded methyl group (signal 1 in Fig. 7) is –2.9 ppm, whereas chemical shift of the comparatively less shielded group is –1.4 ppm. Such a large difference in chemical shift is attributed to the presence of only one methyl group at the deepest core of the cavity.

In the NOESY NMR spectrum of the complex (Fig. 8 and 9), correlations existed between all six methyl groups and H_g of the host. The three most shielded methyl groups (signals 1, 2 and 3) showed NOE interactions exclusively with H_g, while other three methyl groups of the guest showed NOE interactions with H_d and H_e of the host as well. The more shielded signals are expected to be deeper in the cavity and NOE interaction specifically with H_g of the host confirms that the guest exists in the orientation shown in Fig. 10. Note that only one of the geminal methyl groups is

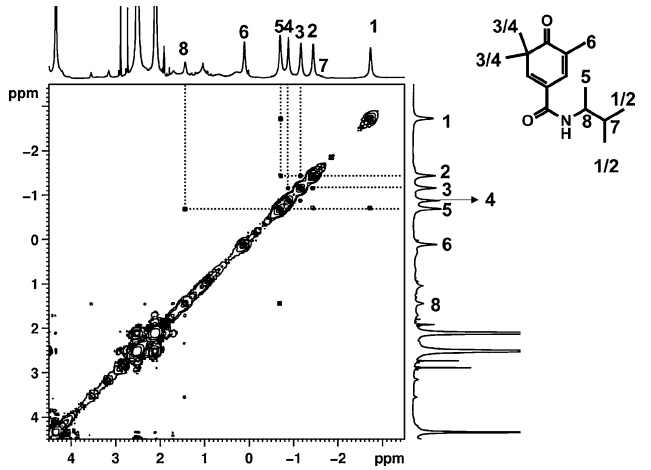

Fig. 8 Partial COSY NMR spectrum (300 MHz, D_2O, 2.5×10^{-3} M **2**, 5×10^{-3} M OA, 5×10^{-2} M sodium tetraborate) of **2**@OA_2. Correlations between the guest signals are marked with dotted lines.

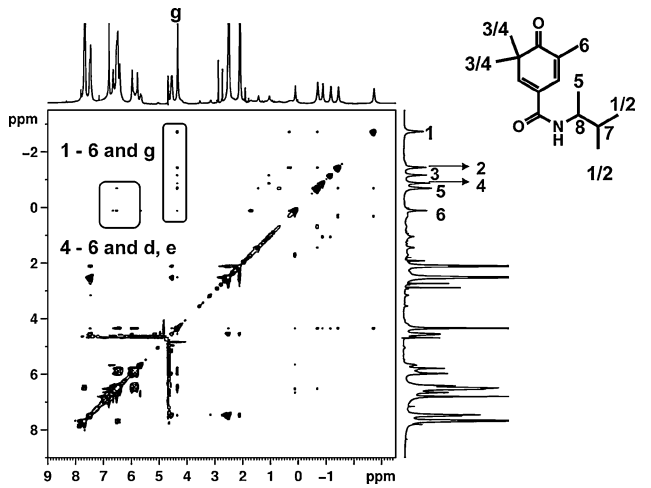

Fig. 9 NOESY NMR spectrum (500 MHz, D_2O, 2.5×10^{-3} M **2**, 5×10^{-3} M OA, 5×10^{-2} M sodium tetraborate, 0.5 s mixing time) of **2**@OA_2. Correlations between the guest methyl signals and host signals are highlighted.

directed to the center of the cavity, based on the chemical shifts of the two methyl groups of –2.9 ppm and –1.4 ppm.

Based on the above analyses of the NMR spectra, we visualize the OA complexes of **1** and **2** to have structures shown in Fig. 11. In the excited state time scale (excited singlet and triplet) these structures are expected to be stationary and not undergo assembly and disassembly of the capsular complex. In addition, guest molecules within the OA capsule are not expected to have as much freedom when they are free in the absence of OA in solution.

Photochemistry of guest@OA_2 complexes

The cyclization reaction of tropolone ether **1** was carried out in acetonitrile and as OA complex at 298 and 278 K for 5 min. The photoproducts were extracted with chloroform and analyzed by gas chromatography using a Supelco β-dex 325 chiral column. When irradiated in acetonitrile, the reaction was racemic—presence of the chiral auxiliary did not have any effect on the reaction. Octa acid bound **1** yielded photoproducts **3** and **3a**

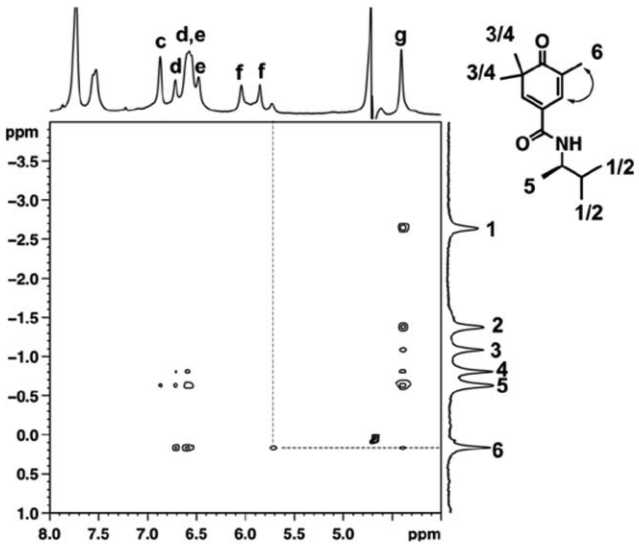

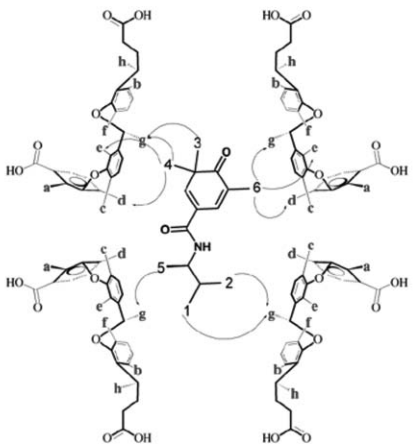

Fig. 10 Top: partial NOESY NMR spectrum (500 MHz, D_2O, 2.5×10^{-3} M **2**, 5×10^{-3} M OA, 5×10^{-2} M sodium tetraborate, 0.5 s mixing time) of **2**@OA_2. Distinct correlations between the guest methyl signals '1–6′ and H_g of the host, and guest methyl signals '4–6′ and H_g of the host can be seen and is shown in the bottom figure. Intramolecular NOE interaction between signal '6′ and the olefin signal at 5.7 ppm is connected with dotted lines.

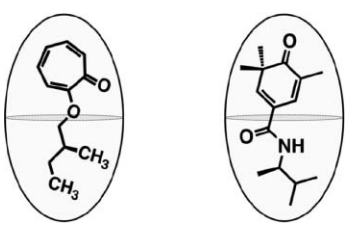

Fig. 11 Cartoon representation of the 2 : 1 complexes formed between host OA and guests **1** (left) and **2** (right), respectively.

with de of 17% (A) at 298 K and 35% (A) at 278 K (the first photoproduct signal in GC analysis was arbitrarily assigned as A and the second signal was assigned B; no attempt was made to ascertain the absolute configuration of the photoproducts). This result confirmed that although the substrate tropolone and the chiral moiety were bound to two different OA molecules that make

up the capsule, chiral induction is possible. It also suggested that although the OA capsule is large enough to accommodate the entire guest and allow movement of the bound guest, yet is small enough to restrict the motion to force interaction between the chiral auxiliary and reactant parts of the molecule.

Results obtained with dienone **2** were also encouraging. As mentioned in Scheme 4, the oxa-di-π-methane rearrangement of **2** occurs to yield two photoproducts. In homogeneous solvents like acetonitrile, the reaction yields equal amounts of both the products even in the presence of the chiral auxiliary because of the large freedom of rotation present in such conditions. Photochemical reaction was carried out by irradiating **2** in acetonitrile and as OA complex at 278 K and 298 K. When **2** was irradiated as acetonitrile solution and the products were analyzed by gas chromatography using a Supelco β-dex 325 chiral column; the formation of 3% excess of one diastereoisomer was observed. When **2**@OA_2 complex was irradiated and the photoproducts analyzed, formation of 36% excess of one diastereoisomer at 278 K (17% at 298 K) was observed.

Both in the case of tropolone ether **1** and dienone **2**, chiral auxiliary does not affect the reaction when it is carried out in a homogeneous solution. This is because of the rotational freedom experienced by the chiral auxiliary in isotropic media. When the molecule is included in a supramolecular host, the role of the host molecule is to rigidly contain the guest inside the cavity. Depending on the orientation of the guest, and the proximity of the chiral auxiliary to the substrate, preference for cyclization reaction along one face of the molecule can be achieved.

Negative results of some consequence

Based on the results of **1**@OA_2 complex, tropolone derivatives bearing a few more chiral auxiliaries (Scheme 5) were synthesized and their binding properties with octa acid and their photochemistry were explored. NMR titration studies with **5** and octa acid confirmed that **5** did not form a strong complex with octa acid. While bound guest signals were observed at 2 : 0.25 (host–guest) ratio, guest signals were not evident in the NMR spectrum of the complex in 2 : 1 ratio (see ESI for NMR spectra).† It may be a result of rapid exchange of the guest or weak binding, but even the free (unbound) guest signals were not recorded. Similarly, the ester derivative **6** did not form a strong complex with octa acid. Only the octa acid signals were observed in the titration NMR spectra of octa acid–**6** mixture (see ESI for NMR spectra).† Although at host–guest ratio 2 : 0.25 and 2 : 0.5 equiv., broadening of H_c and H_d signals of octa acid was observed, guest signals were not seen. NOESY NMR of the complex recorded at 278 K (5 °C) also showed no host–guest interactions. Thus, the NMR data is consistent with either a weak complexation between **5** and **6** with OA or/and rapid equilibrium in the NMR time scale between non-complexed and complexed guest and host. Irradiation of octa acid solutions of either guests **5** or **6** showed no selectivity in the cyclization reaction. The observed negative results could be due to the fact that either **5** and **6** did not complex to OA or the complexes were extremely weak. It is quite likely that photoreactions result from non-complexed undissolved microparticulates in solution. The absence of any NMR signals for either complexed or free guest molecules are consistent with this possibility. Since the photochemical results were not promising no variable temperature NMR experiments were carried out.

Another tropolone ether studied was the (–)-menthol ether of tropolone, **7** (Scheme 5).[28] Based on ^{1}H NMR spectra of the complex, the formation of a 2 : 1 complex between octa acid and **7** was confirmed. ^{1}H NMR spectrum of the octa acid complex of **7** recorded at 298 K is shown in Fig. 12 (top). Characteristic high field shifted guest signals and multiply split host signals were readily observed. Guest signals were generally broad and were spread from 0.5 ppm to –1.5 ppm and between –2.5 to –3.2 ppm. However, unlike most other guests studied with OA, intensities of the guest signals of **7** were low and signals were broad. Even upon cooling to 278 K (Fig. 12, bottom), the characteristics of the guest signals did not improve. Broadening of the octa acid signals at 278 K when compared to the spectrum recorded at 298 K suggested that upon cooling, the conformational dynamics of the guest inside the cavity and interconversion between several different guest orientations were slower. The above data is also consistent with the postulate that the kinetic stability of **7**@OA complex is poor compared with **1**@OA_2.

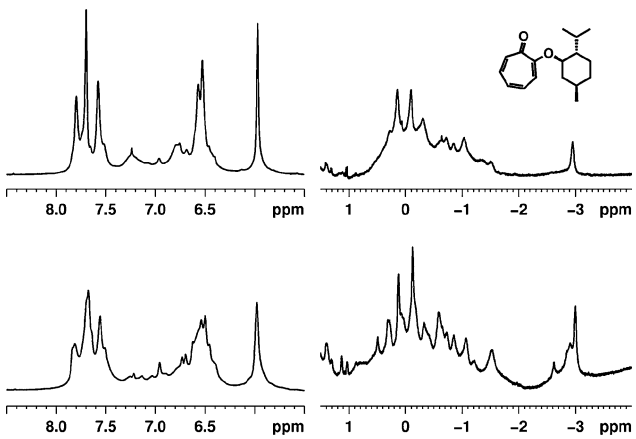

Fig. 12 ^{1}H NMR spectra of **7**@OA_2 (500 MHz, D_2O, 2.5×10^{-3} M **7**, 5×10^{-3} M OA, 5×10^{-2} M sodium tetraborate) recorded at 298 K (top) and at 278 K (bottom). Intensity of the high field region (spectrum on the right) is greater than the intensity of the low-field region (spectrum on the left).

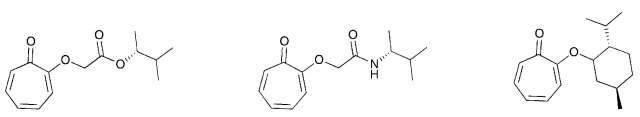

Scheme 5 Structures of tropolone derivatives appended to chiral ester (**5**), chiral amide (**6**) and ether (**7**).

Photochemical behaviour of **7** bound to octa acid was similar to the reaction in acetonitrile. Racemic mixture of photoproducts was observed. Unlike **5** and **6** that did not bind at all, **7** formed a relatively stable complex with octa acid. In spite of that the photoreaction yielded a racemic product mixture. Results observed with four tropolone ethers (**1**, **5**, **6** and **7**) suggest that for the chiral auxiliary to be effective the host–complex must be

strong and the structural flexibility of the guest must be restricted than in solution.

Conclusion

Moderately diastereoselective photoreactions of **1** and **2** were observed when they are complexed to a synthetic cavitand. The observed results suggest that factors like substituent effects and weak interactions between octa acid and the guests influenced the outcome of the reaction. Strong binding nature of the two guests to OA is likely to play a major role in the observed selectivity. But exact mechanism of chirality transfer is not clear. Presently, further study is required to establish the role of the chiral auxiliary and the influence of OA in the diastereoselective reactions. The results presented here establish that OA has the ability to confine the guest in its cavity and consequently, diastereoselective reactions can be carried out using octa acid as host.

Experimental

Synthesis of compounds **1**, and **2**, and their photoproducts were reported earlier.[28] The procedure for the synthesis of compounds **5**, **6** and **7** is given below. The sequence of reactions followed is outlined in Schemes 6 and 7.

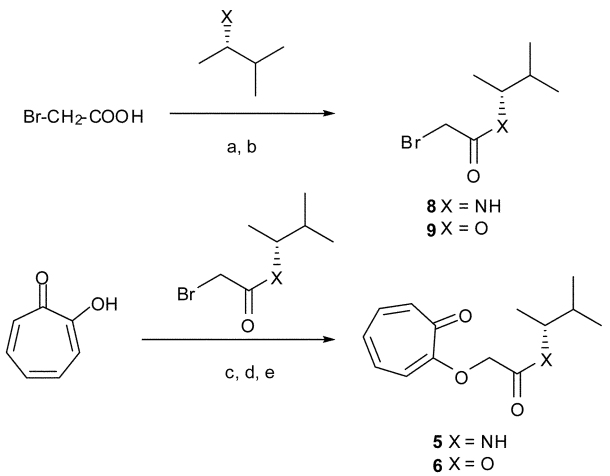

Scheme 6 Sequence of reactions used to synthesize reactants **5** and **6**.

Synthesis of (*R*)-2-bromo-*N*-(3-methylbutan-2-yl)ethanamide (8) and (*R*)-3-methylbutan-2-yl-2-bromoethanoate (9)

A nitrogen bubbled solution of *N*-(3-dimethylaminopropyl)-*N*′-ethylcarbodiimide hydrochloride (EDC·HCl) in methylene chloride was stirred with bromoacetic acid (1 equiv.) and either (*R*)-3-methyl-2-butanol or (*R*)-3-methylbutan-2-amine (1.2 equiv.) at room temperature for 24 h. The organic layer was washed with water, aqueous Na_2CO_3 solution and brine, dried with anhydrous sodium sulfate and concentrated. The crude ester was used as such for the next step.

Synthesis of *N*-((*R*)-3-methylbutan-2-yl)-2-((1*E*,3*Z*,5*Z*)-7-oxocyclohepta-1,3,5-trienyloxy)ethanamide (5)/(*R*)-3-methylbutan-2-yl 2-((1*E*,3*Z*,5*Z*)-7-oxocyclohepta-1,3,5-trienyloxy)ethanoate (6)

Tropolone (1 equiv.) was dissolved in acetonitrile and anhydrous NaY (activated at 500 °C for 5 h) and anhydrous potassium carbonate were added. The mixture was heated to reflux and stirred at reflux for 60 min. Intermediate **8**/**9** was added in one portion to the reaction mixture. After 16 h at reflux, the insoluble content was filtered and the acetonitrile was distilled. Pure **5**/**6** was obtained by column purification (silica gel, hexanes and chloroform).

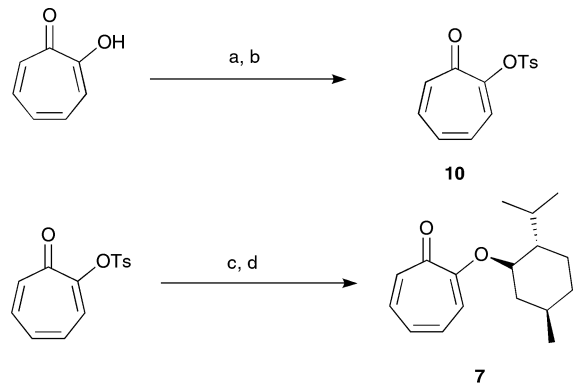

Scheme 7 Sequence of reactions used to synthesize reactant **7**.

Synthesis of tropolone-4-methylbenzenesulfonate (10)

Tropolone (1 equiv.) was dissolved in minimum amount of pyridine (1 g in 6–8 mL) and recrystallized *para*-toluenesylfonyl chloride (TsCl, 1.2 equiv.) was added to the solution. The turbid solution was stirred for 24 h at room temperature and filtered. The precipitate was dried and used in the next step as obtained.

Synthesis of (2*E*,4*Z*,6*Z*)-2-((1*R*,2*S*,5*R*)-2-isopropyl-5-methylcyclohexyloxy)cyclohepta-2,4,6-trienone (7)

(–)-Menthol (1 equiv.) was dissolved in THF and gradually potassium *tert*butoxide (1.1 equiv.) was added with stirring. After 15 min, **10** (1 equiv.) was added as solid in one portion to the reaction slurry. The clear solution turned dark brown instantly. It was stirred at room temperature for 24 h. The reaction was quenched by adding ice-cold water. THF was distilled and the organics were extracted with three portions of chloroform. The organic layer was washed with brine, dried with anhydrous sodium sulfate, and concentrated. Flash column chromatography (silica gel, hexanes, ethyl acetate) was employed to isolate pure **7**.

Protocol for preparation and photolysis of complex, and isolation and analysis of products

General methods. All NMR experiments were carried out with Bruker Avance Spectrometers at 298 K unless mentioned otherwise. 1D TOCSY spectra were recorded with 0.12 s mixing time; NOESY spectra were recorded with 0.5 s mixing time. Photolysis of the substrates were carried out using a 450 watt

medium pressure Hg lamp. All solutions were bubbled with nitrogen for 15 min prior to photolysis.

Procedure for NMR titration experiments. Octa acid solution (0.6 mL, 10^{-3} M OA in buffered D_2O) was taken in an NMR sample tube and its ^1H NMR spectrum was recorded. Stock solution of the guest was prepared in CD_3CN. Aliquots of the guest solution were added to the octa acid solution, usually in 2.5 μL increments, and the NMR spectrum of the complex was recorded after addition.

Preparation of the complex with guests 1, 2, 5 and 7. A stock solution of the guest was prepared in CD_3CN. An aliquot of the stock solution was transferred to a sample vial and the solvent was evaporated in a stream of air with gentle warming. Octa acid solution (in buffered D_2O) was added to the guest and the vial was sonicated for ~5 min. The solution was then transferred to an NMR tube and sealed. NMR spectrum of the complex was recorded. The NMR sample solution was used for irradiation experiments.

Photolysis experiments. A solution of octa acid–guest complex was sealed in a Pyrex test tube with a septum and was purged with nitrogen for 15 min prior to irradiation. The solution was cooled in an ice-water bath held at 278 K and equilibrated for 15 min. A medium pressure Hg lamp was used to irradiate the complexes. All tropolone ether solutions (**1**, **5** and **7**) were irradiated for 2–4 min while solution of **2** was irradiated for 30–45 min. The irradiation period was determined by comparison with irradiation of acetonitrile solutions of the guests. After irradiation, octa acid solutions were extracted with two portions of chloroform. The chloroform layer was analyzed by GC using a chiral column (Supelco β-DEX 325 capillary column). GC conditions and retention times of the photoproducts for each substrate are given below. The enantiomeric excess (ee) of a reaction is given by the ratio (A − B/A + B) × 100, where A refers to the area under the first peak of the product and B refers to the area under the second peak.

Analyses conditions for the diastereomeric excess of the photoproducts of 1, 2, 5 and 7. GC: HP 5890 series fitted with a chiral column (Supelco -dex 325 [phase, non-bonded; 25% 2,3-di-O-methyl-6-O-TBDMS–cyclodextrin in SPB-20 poly(20% phenyl/80% dimethyl siloxane)]).

1. Initial Temperature 100 °C for 2 min; initial ramp 0.5 °C min^{-1} till 125 °C; hold at 125 °C for 2 min, ramp at 10 °C min^{-1} till 200 °C. Retention time of photoproducts 39.9 min and 40.5 min.

2. Initial Temperature 120 °C for 2 min; initial ramp 5 °C min^{-1} till 160 °C; hold at 160 °C for 5 min, ramp at 2 °C min^{-1} till 200 °C. Retention time of photoproducts 30.6 min and 31.1 min.

5. Initial Temperature 60 °C for 1 min; initial ramp 2 °C min^{-1} till 200 °C; hold at 200 °C for 10 min. Retention time of photoproducts 46.6 min and 48 min.

6. Initial Temperature 80 °C for 1 min; initial ramp 3 °C min^{-1} till 160 °C; hold at 160 °C for 30 min, ramp at 2 °C min^{-1} till 200 °C. Retention time of photoproducts 53.5 min and 54.3 min.

7. Initial Temperature 120 °C for 5 min; ramp 5 °C min^{-1} till 200 °C. Retention time of photoproducts 25.6 min and 26.2 min.

Acknowledgements

VR thanks the National Science Foundation, USA (CHE-0213042 and CHE-0531802) and BCG the National Institute of Health (RO1 GM074031) for financial support.

References

1 Y. Inoue and V. Ramamurthy, *Chiral Photochemistry*, Marcel Dekker, New York, 2004.
2 Y. Inoue, *Chem. Rev.*, 1992, **92**, 741–770.
3 H. Rau, *Chem. Rev.*, 1983, **83**, 535–547.
4 J. Sivaguru, A. Natarajan, L. S. Kaanumalle, J. Shailaja, S. Uppili, A. Joy and V. Ramamurthy, *Acc. Chem. Res.*, 2003, **36**, 509–521.
5 J. Sivaguru, J. Shailaja and V. Ramamurthy, in *Handbook Of Zeolite Science and Technology*, ed. S. M. Auerbach, K. A. Carrado and P. K. Dutta, Marcel Dekker, New York, 2003, pp. 515–589.
6 J. R. Scheffer and W. Xia, *Top. Curr. Chem.*, 2005, **254**, 233–262.
7 J. R. Scheffer, in *Chiral Photochemistry*, ed. Y. Inoue and V. Ramamurthy, Marcel Dekker, New York, 2004, pp. 463–483.
8 F. Toda, K. Tanaka and H. Miyamoto, in *Understanding and Manipulating Excited-State Processes*, ed. V. Ramamurthy and K. S. Schanze, Marcel Dekker, New York, 2001, vol. 8, pp. 385–425.
9 K. Tanaka and F. Toda, in *Organic Solid State Reactions*, ed. F. Toda, Kluwer, New York, 2002, pp. 109–157.
10 W. G. Dauben, K. Koch, S. L. Smith and O. L. Chapman, *J. Am. Chem. Soc.*, 1963, **85**, 2616–2621.
11 O. L. Chapman and D. J. Pasto, *J. Am. Chem. Soc.*, 1960, **82**, 3642–3648.
12 H. Hart, P. M. Collins and A. J. Waring, *J. Am. Chem. Soc.*, 1966, **88**, 1005–1011.
13 H. Hart and R. K. J. Murray, *J. Org. Chem.*, 1970, **35**, 1535–1542.
14 C. L. D. Gibb and B. C. Gibb, *J. Am. Chem. Soc.*, 2004, **126**, 11408–11409.
15 B. C. Gibb, in *Organic Nanostructures*, ed. J. L. Atwood and J. W. Steed, VCH Verlag GmbH & Co., Weinheim, 2008, pp. 291–304.
16 L. S. Kaanumalle, C. L. D. Gibb, B. C. Gibb and V. Ramamurthy, *J. Am. Chem. Soc.*, 2005, **127**, 3674–3675.
17 L. S. Kaanumalle, C. L. D. Gibb, B. C. Gibb and V. Ramamurthy, *J. Am. Chem. Soc.*, 2004, **126**, 14366–14367.
18 A. Natarajan, L. S. Kaanumalle, S. Jockusch, C. L. D. Gibb, B. C. Gibb, N. J. Turro and V. Ramamurthy, *J. Am. Chem. Soc.*, 2007, **129**, 4132–4133.
19 S. Koodanjeri and V. Ramamurthy, *Tetrahedron Lett.*, 2002, **43**, 9229–9232.
20 S. Koodanjeri, A. Joy and V. Ramamurthy, *Tetrahedron*, 2000, **56**, 7003–7009.
21 J. Shailaja, S. Karthikeyan and V. Ramamurthy, *Tetrahedron Lett.*, 2002, **43**, 9335–9339.
22 A. Nakamura and Y. Inoue, *J. Am. Chem. Soc.*, 2003, **125**, 966–972.
23 C. Yang, G. Fukuhara, A. Nakamura, Y. Origane, K. Fujita, D.-Q. Yuan, T. Mori, T. Wada and Y. Inoue, *J. Photochem. Photobiol., A*, 2005, **173**, 375–383.
24 K. Vizvardi, K. Desmet, I. Luyten, P. Sandra, G. Hoornaert and E. V. der Eycken, *Org. Lett.*, 2001, **3**, 1173–1175.
25 C. L. D. Gibb, A. K. Sundaresan, V. Ramamurthy and B. C. Gibb, *J. Am. Chem. Soc.*, 2008, **130**, 4069–4080.
26 A. K. Sundaresan and V. Ramamurthy, *Photochem. Photobiol. Sci.*, 2008, **7**, 1555–1564.
27 A. K. Sundaresan and V. Ramamurthy, *Org. Lett.*, 2007, **9**, 3575–3578.
28 A. Joy, L. S. Kaanumalle and V. Ramamurthy, *Org. Biomol. Chem.*, 2005, **3**, 3045–3053.